Detection meeting control: Unstable steady states in high-dimensional nonlinear dynamical systems

Huanfei Ma,[1,2] Daniel W. C. Ho,[3] Ying-Cheng Lai,[4] and Wei Lin[2,5,*]

[1]*School of Mathematical Sciences, Soochow University, Suzhou 215006, China*
[2]*Center for Computational Systems Biology, Fudan University, Shanghai 200433, China*
[3]*Department of Mathematics, City University of Hong Kong, Hongkong, China*
[4]*School of Electrical, Computer, and Energy Engineering, Arizona State University, Tempe, Arizona 85287-5706, USA*
[5]*School of Mathematical Sciences and SCMS, Fudan University, Shanghai 200433, China*

We articulate an adaptive and reference-free framework based on the principle of random switching to *detect and control* unstable steady states in high-dimensional nonlinear dynamical systems, without requiring any *a priori* information about the system or about the target steady state. Starting from an arbitrary initial condition, a proper control signal finds the nearest unstable steady state adaptively and drives the system to it in finite time, regardless of the type of the steady state. We develop a mathematical analysis based on fast-slow manifold separation and Markov chain theory to validate the framework. Numerical demonstration of the control and detection principle using both classic chaotic systems and models of biological and physical significance is provided.

PACS number(s): 05.45.Gg, 05.45.Jn

I. INTRODUCTION

Controlling nonlinear dynamical systems is a challenging task with applications in many fields. In a real world situation a mathematical model of the underlying system is not always available, so one must rely on measured data or time series to realize control. For low-dimensional chaotic systems, the problem of data-based control has largely been solved, thanks to the seminal contribution of Ott, Grebogi, and Yorke (OGY) [1]. In particular, the OGY methodology enables stabilization of a chaotic trajectory about one of the infinite number of unstable periodic orbits (UPOs) embedded in the underlying chaotic invariant set by using small control perturbations. Control of high-dimensional nonlinear systems, however, remains an outstanding problem, due to the many different types of complex behaviors that such systems can exhibit. To achieve control, it is necessary to determine the target UPO. In the past three decades, various methods to calculate UPOs from system equations were proposed [2–6]. There has also been a great deal of effort in detecting UPOs based on measured data [7–12]. In most previous works, detecting UPOs and controlling chaos were done separately.

The goal of our work is to *develop a single framework* to detect *and* control unstable steady states (USSs) without requiring knowledge of the underlying system or the target USS. This problem is particularly relevant to systems biology, where high-dimensional gene regulatory networks (GRNs) typically possess a number of USSs that are important for system functionality. In fact, USSs in GRNs are closely related to the fundamental concept of biological robustness [13] and have implications, e.g., in designing therapeutically effective strategies to treat tumor cells [14–16]. Recently, it was demonstrated experimentally using synthetic biological circuits that USSs play an essential role in fundamental phenomena such as stochastic cell fate determination [17].

From a dynamical point of view, in situations where there are multiple attractors, the stable manifold of a USS is nothing but the boundary separating distinct basins of attraction. In systems biology, different attractors correspond to distinct cell fate, e.g., a normal cell or a tumor cell. When a trajectory comes near the stable manifold, any random disturbance can cause the system to approach a completely different attractor [17], leading to stochastic cell fates. To be able to detect and control the USS is thus key to engineering and manipulating gene regulatory networks to achieve desired cell fate.

There are methods to stabilize USSs based on proportional feedback control [18–20], which require knowledge about the mathematical model of the underlying dynamical system. If such information is not available, the precise location of a desired USS in the phase space would be needed as a reference to enable control. A number of control techniques have been proposed, such as those based on derivative feedback, low- or high-pass filters, and delayed feedback. These techniques, when implemented in an adaptive manner, are capable of locating and stabilizing some particular types of USSs [21–27], but success still relies largely on information about the USSs, such as the number of real positive eigenvalues of the Jacobian matrix [28] or the type of the USS (e.g., saddle versus nonsaddle type) [28–30]. In real world systems, particularly in dynamical systems of significant biological and/or physical interest with multistability [17,31–37], neither the exact models nor the accurate coordinates of the reference point are known *a priori*. Developing a model-independent and reference-state free framework to *simultaneously* detect and control USSs is thus an outstanding problem with broad interest.

In this paper, we articulate an effective framework based on random switching [38,39] and adaptive control to precisely locate unknown USSs in finite time with minimal energy consumption. Our scheme is completely model free and it does not require any *a priori* information about any USS in the system. We are able to obtain rigorous mathematical support for the control and detection framework, and we present numerical demonstration using a classic nonlinear

---

*To whom correspondence should be addressed: wlin@fudan.edu.cn.

dynamical system, and systems of significant biological and physical interest, including a high-dimensional GRN and an infinite-dimensional time-delayed system.

In Sec. II, we describe the basic principle of random switching control and develop a mathematical theory using the classic chaotic Lorenz system as a vehicle to gain insights into detection and control of USSs. In Sec. III, we demonstrate the working of our random switching framework with examples from physics and biology. In Sec. IV, we present conclusions and discussions.

II. FRAMEWORK OF RANDOM SWITCHING CONTROL

We formulate our control and detection framework for systems described by $\dot{x} = f(x)$, where the n-dimensional state variable is $x = [x_1, \dots, x_n]^\top \in \mathbb{R}^n$ and the smooth vector field is $f(x) = [f_1(x), \dots, f_n(x)]^\top$. The aim is to design a noninvasive controller $u(x)$ to detect and stabilize any unknown USS, denoted by $x^* = [x_1^*, \dots, x_n^*]^\top$. The system under control can be written as

$$\dot{x} = f(x) + u(x), \tag{1}$$

which would converge asymptotically to x^* such that $f(x^*) = 0$ and $u(x^*) = 0$. We choose the following general proportional feedback controller:

$$u(x) = K \cdot [y - g(x)], \tag{2}$$

where the diagonal matrix $K = \text{diag}(k_1, \dots, k_n)$ characterizes the coupling between the system and the controller, $y = [y_1, \dots, y_n]^\top \in \mathbb{R}^n$ represents a reference point of the target USS, and $g(x) = [g_1(x), \dots, g_n(x)]^\top$ is a measurement function or an output of the controlled system. For a real-world system, it is practically infeasible to control every dynamical variable. However, as our mathematical analysis below indicates, controlling every component is unnecessary—an appealing feature of our control scheme. Without loss of generality, we consider the challenging case where only one dynamical variable is subject to control, i.e., we set the matrix K as $k_i = k \neq 0$ and $k_j = 0$ for $j \neq i$. To search for any unknown USS, we employ the following random switching rule to adaptively adjust the reference value y_i:

$$\dot{y}_i = \omega(t)[g_i(x) - y_i], \tag{3}$$

where $\omega(t) \in \mathbb{R}$ is a switching parameter determined by $\omega(t) = \omega_{\sigma(t)}$ for $t \in \mathcal{I}_n \triangleq [n\Delta T, (n+1)\Delta T)$ $(n = 0, 1, 2, \cdots)$, ΔT is the duration of the switching time, and $\sigma(t)$ in each time interval $\mathcal{I}_n$ can be regarded as a discrete random variable taking its values from the index set $\{+, -\}$. The corresponding probability is

$$\mathbb{P}\{\sigma(t) = +|t \in \mathcal{I}_n\} = \mathbb{P}\{\sigma(t) = -|t \in \mathcal{I}_n\} = 1/2. \tag{4}$$

We see that ω_+ (ω_-) takes on positive (negative) values that can be adjusted to yield optimal searching.

To motivate a mathematical analysis of our control and detection framework, we perform a benchmark study using the classic chaotic Lorenz system [40]: $\dot{x}_1 = \sigma(x_2 - x_1)$, $\dot{x}_2 = x_1(\rho - x_3) - x_2$, and $\dot{x}_3 = x_1x_2 - \beta x_3$, for $\sigma = 10$, $\beta = 8/3$, and $\rho = 28$. There are three USSs: one of the saddle type denoted as $P_1(0,0,0)$, and the other two being focuses denoted

as $P_{2,3}(\pm\sqrt{[\beta(\rho-1)]}, \pm\sqrt{[\beta(\rho-1)]}, \rho-1)$, as shown in Fig. 1(a). The controlled Lorenz system is

$$\dot{x}_1 = \sigma(x_2 - x_1), \quad \dot{x}_2 = x_1(\rho - x_3) - x_2 + k(y - x_2),$$
$$\dot{x}_3 = x_1x_2 - \beta x_3, \quad \dot{y} = \omega(t)(x_2 - y), \tag{5}$$

where the measurement function is chosen to be $g(x) = x_2$ and the controller $k(y - x_2)$ with the coupling strength $k_2 = k$ is introduced into the second variable of the Lorenz system. Figure 1(b) shows the behavior of the controlled system, where one control realization for each initial condition set is depicted. We see that all USSs can be controlled and detected. Under control, each USS may be regarded as an "attractor" with a basin. Figure 1(c) shows the approximate distribution of the basin volume for each USS. According to the recently developed basin stability theory [41,42], the extensive basin implied in Fig. 1(c) indicates that the controller is quite robust against perturbation. Moreover, we find that, when the initial condition is chosen from the interval between P_2 and P_3, the controlled system will converge to one of the USSs with probability 1, and the probability to converge to a specific USS is inversely proportional to the distance between it and the initial condition. Note that, if the random variable $\omega(t)$ in the controlled Lorenz system is fixed (either ω_+ or ω_-), our control method reduces to the method based on deterministic stable or unstable low-pass filters [43]. The results are shown in Figs. 1(d) and 1(e). In this case, however, not all USSs can be stabilized simultaneously with a single low-pass filter. Intuitively, one might regard our random switching scheme as some kind of averaging process of the two types of low-pass filtering. However, it is difficult to understand the key feature of our framework that the probability of convergence to an USS approaches unity. In the following we provide a mathematical analysis to understand the counterintuitive phenomenon.

First, we note that, in spite of random switching, our adaptive method possesses a fast-slow manifold separation [27], due to the fact that $|\omega| \ll k$ for sufficiently large k. The rate of change in the reference signal y is thus much smaller than that of the dynamical variable x, and dissipation introduced by the controller will drive the system to a low-dimensional subspace. As a result, starting from an initial condition, within a short time period the controlled system approaches a hypersurface defined by $\dot{x}_i = 0$ $(i = 1, 2, \dots, n)$. When this occurs, the slow variable y evolves according to Eq. (3) and the controlled variable x preserves the relation $\dot{x}_i = 0$ $(i = 1, 2, \dots, n)$. On the hypersurface, Eq. (3) becomes

$$\dot{y} = \omega(t)[h(y) - y], \tag{6}$$

where $h(y)$ is a smooth function [the index i in Eq. (3) has been omitted for simplicity]. An example of the fast-slow manifold separation for the controlled Lorenz system is shown in Fig. 2, with the corresponding hypersurface given explicitly by $x_2 - y = h(y) - y$, where $y = x_2 - [(\rho - 1)x_2 - x_2^3/\beta]/k$.

Without loss of generality, we assume that the dynamical system on the hypersurface is nondegenerate, i.e., the algebraic equation $h(y) - y = 0$ has m distinct roots in the order $y_1^* < y_2^* < \cdots < y_m^*$, corresponding to the m USSs in the uncontrolled system, respectively. In addition, we assume $h'(y_i^*) - 1 \neq 0$ for $i = 1, 2, \dots, m$. Now consider an initial condition between two adjacent fixed points, y_1^*
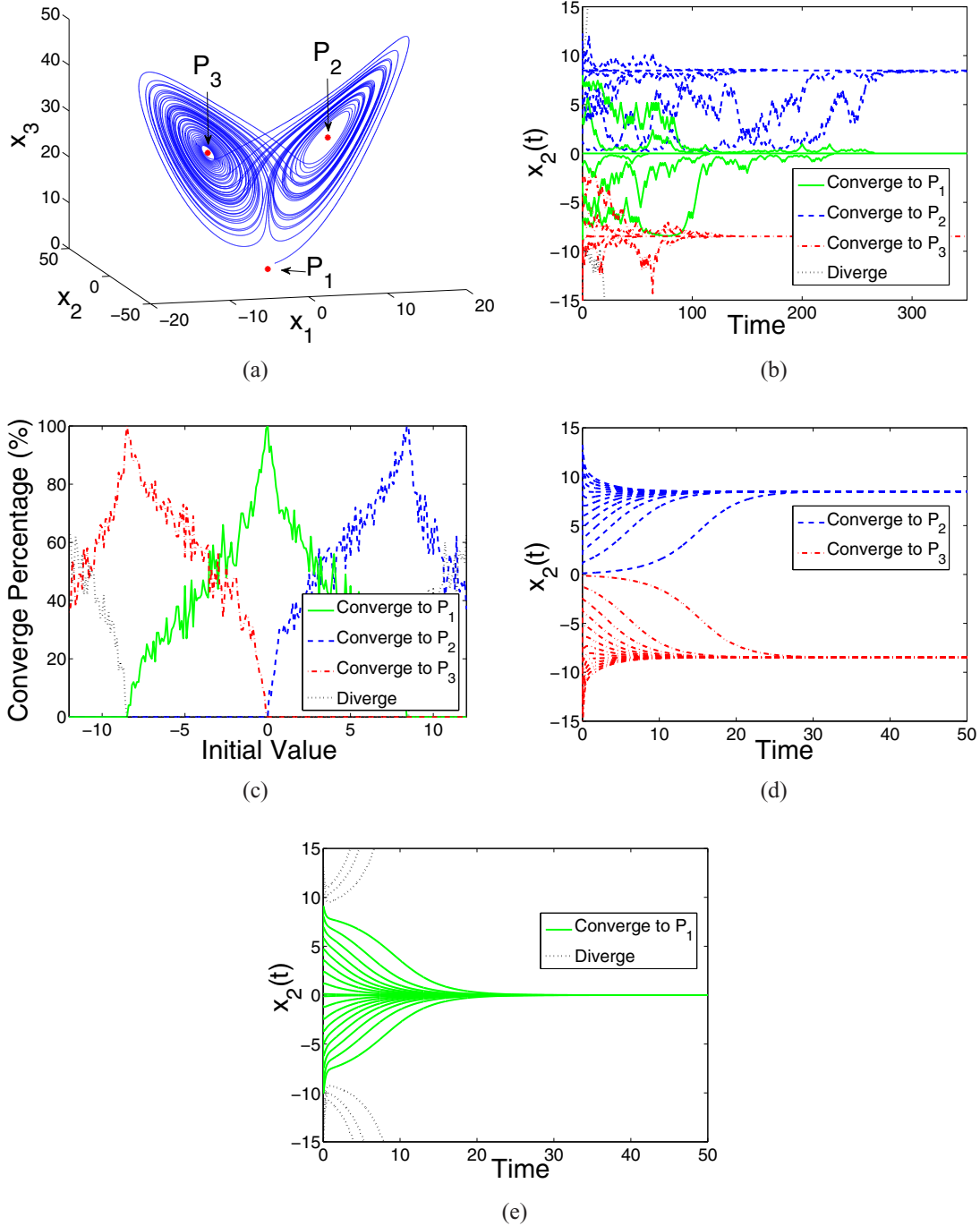
FIG. 1. (Color online)   (a) A chaotic attractor of the Lorenz system with three USSs (highlighted). (b) Time series $x_2(t)$ of the controlled Lorenz system starting from different initial conditions. (c) Approximate distributions of the "basin" volumes of the USSs. The probability of convergence to each USS is calculated using 100 independent control realizations. For the previous method, the time series $x_2(t)$ is used: $\omega(t) \equiv \omega_+$ (d) and $\omega(t) \equiv \omega_-$ (e), where $\omega_+ = 1$, $\omega_- = -1$, $k = 130$, and time window $\Delta T = 1$. The initial conditions are from the subspace defined by $x_1(0) = x_2(0) = x_3(0) = y_2(0)$.

and y_2^*. The nondegeneracy assumption stipulates that the trajectory follows that determined by $y_0 = y(0) \in (y_1^*, y_2^*)$, where $h(y_1^*) - y_1^* = h(y_2^*) - y_2^* = 0$ such that $h'(y_1^*) > 1$ and $h'(y_2^*) < 1$, as illustrated in Fig. 3(a). For $\omega(t) \equiv \omega_+$ (ω_-), the fixed point y_2^* (y_1^*) is attractive. Let $y_{+1}, y_{+2}, \ldots, y_{+n}, \ldots$ be the system states at each switching instant $n\Delta T$ for the case $\omega(t) \equiv \omega_+$. We have $\lim_{n \to \infty} y_{+n} = y_2^*$, as shown in Fig. 3(b).

Analogously, letting $y_{-1}, y_{-2}, \ldots, y_{-n}, \ldots$ be the corresponding states for the case $\omega(t) \equiv \omega_-$, we have $\lim_{n \to \infty} y_{-n} = y_1^*$, as shown in Fig. 3(c). In our control scheme, $\omega(t) = \omega_{\sigma(t)}$ switches its value between ω_+ and ω_- randomly at each time instant $n\Delta T$ and keeps its value unchanged for the duration ΔT. As a result, the system state $y_n = y(n\Delta T)$ takes on its value from the grid $y_i (i = 0, \pm 1, \pm 2, \ldots)$ stochastically
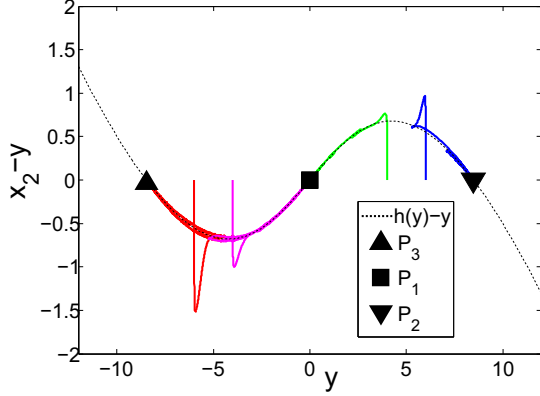
FIG. 2. (Color online) For the controlled Lorenz system, an example of fast-slow manifold separation, where the dotted line is calculated by setting $\dot{x}_1 = \dot{x}_2 = \dot{x}_3 = 0$. Four different trajectories are shown.

with the transition probability

$$\mathbb{P}(y_{n+1} = y_{i+1} | y_n = y_i)$$
$$= \mathbb{P}(y_{n+1} = y_{i-1} | y_n = y_i) = 1/2. \tag{7}$$

The dynamics for y_n can thus be regarded as a random walk without bounds on a one-dimensional grid.

Typically, the process of stabilizing an unknown USS terminates after several successive switches and the variation of $y(t)$ is small: $\text{var}[y(t)] < \delta$ for some given small δ. To obtain a quantitative criterion, we define two stopping regions through
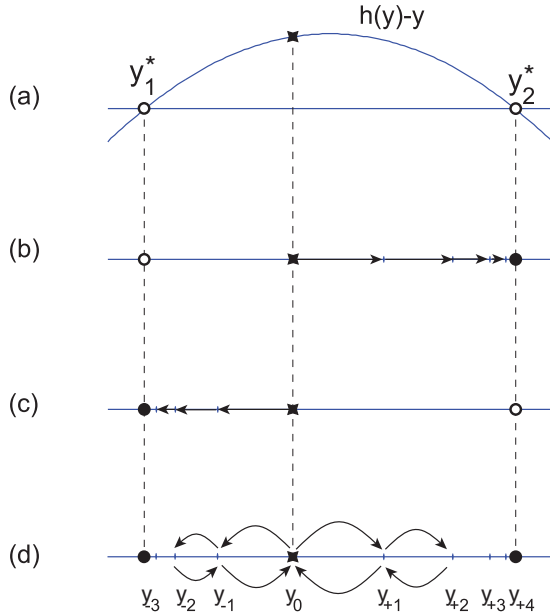
FIG. 3. (Color online) Schematic illustration of random switching control. (a) Function $h(y) - y$ and two neighboring nonde-generated fixed points y_1^* and y_2^*. (b,c) Dynamics of the system $\dot{y} = \omega(t)[h(y) - y]$ starting from initial condition y_0 for $\omega(t) \equiv \omega_+$ and $\omega(t) \equiv \omega_-$, respectively. (d) System dynamics subject to random switching control $\omega(t) = \omega_{\sigma(t)}$, which can effectively be described as a random walk with absorbing boundaries.

two ϵ neighborhoods of the fixed points: $(y_1^*, y_1^* + \epsilon)$ and $(y_2^* - \epsilon, y_2^*)$, where ϵ is related to δ and the stabilization process stops as $y(t)$ enters either region. Under this configuration, $y(t)$ becomes a random walk on a finite grid with two absorbing boundaries: $\{y_{-n_-}, \ldots, y_{-1}, y_0, y_{+1}, \ldots, y_{+n_+}\}$, as shown in Fig. 3(d). Here, $n_+ = \lceil \frac{T_+}{\Delta T} \rceil$, where T_+ is the first time that $y(t)$ enters the right region $(y_2^* - \epsilon, y_2^*)$ if $\omega(t) \equiv \omega_+$, and $n_- = \lceil \frac{T_-}{\Delta T} \rceil$ is similarly defined. Using the theory of Markov chains [44], we arrive at the following lemma, which provides an understanding of the dynamical behaviors of the controlled system.

Lemma. Assume that the system $\dot{y} = \omega(t)[h(y) - y]$ starts from y_0, which is selected from the interval between the two adjacent fixed points y_1^* and y_2^*. Then, (i) this system finally enters one of the absorbing regions of y_i^* with probability 1; (ii) the probabilities of absorption for y_1^* and y_2^* are $n_-/(n_+ + n_-)$ and $n_+/(n_+ + n_-)$, respectively; and (iii) starting from y_0, the expected time to the absorption state is $n_- n_+ \Delta T$.

III. NUMERICAL EXAMPLES

A. Network model of hematopoietic stem cells

We first present results of controlling and detecting USSs in a cellular differentiation network model for hematopoietic stem cells [45]:

$$\dot{x}_1 = e_N - x_1, \quad \dot{x}_2 = \frac{5x_1}{1 + x_1} \frac{1}{1 + x_3^4} - x_2,$$

$$\dot{x}_3 = \frac{5x_4}{1 + x_4} \frac{1}{1 + x_2^4} - x_3, \quad \dot{x}_4 = \frac{e_M}{1 + x_2^4} - x_4,$$

$$\dot{x}_5 = \left(\frac{x_1 x_4}{1 + x_1 x_4} + \frac{4x_3}{1 + x_3} \right) \frac{1}{1 + x_2^4} - x_5,$$

$$\dot{x}_6 = \left(\frac{x_1 x_4}{1 + x_1 x_4} + \frac{4x_2}{1 + x_2} \right) \frac{1}{1 + x_3^4} - x_6, \tag{8}$$

where x_2 and x_3 represent the expression levels of two lineage-specific counteracting suppressors Gfi-1 and Egr(1,2), respectively, which are activated by their transcription factors x_1 and x_4 and regulate the downstream genes x_5 and x_6. This model in fact describes the interplay between the
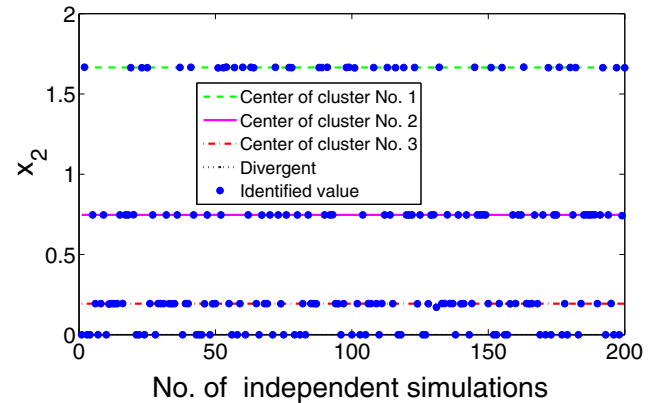
FIG. 4. (Color online) Clusters formed in executing random switching control for the cell system (8), where the coupling strength is $k_2 = 8$ and other parameters are $\Delta T = 10$ and $\omega_\pm = \pm 1$.

TABLE I. Coordinates of the USSs of system (8) and the corresponding estimated errors.

Approximated coordinates of the USSs		Error
U_1	(0.5, 1.66, 0.03, 0.06, 0.02, 2.53)	$O(10^{-4})$
U_2	(0.5, 0.75, 1.05, 0.38, 1.69, 0.83)	$O(10^{-4})$
U_3	(0.5, 0.19, 1.66, 0.50, 2.69, 0.10)	$O(10^{-5})$

two suppressors during cellular differentiation for neutrophil and macrophage cell fate choices, which is a paradigmatic model for characterization of USSs in biological networks [46,47]. Setting parameters as $e_M = e_N = 0.5$, we apply our random switching control to x_2, an experimentally accessible dynamical variable [45]. A representative result is shown in Fig. 4, where 100 independent control runs are carried out and the initial value of x_2 is chosen randomly from the interval [0,1]. We see that the controlled values of x_2 form four clusters, where the convergent points about the three USSs are indicated as clusters 1–3 and the divergent cases are marked by the dots on the line $x_2 = 0$. Calculating the center of each cluster of the convergent points, we obtain the approximate locations of the USSs, as listed in Table I, where U_1 and U_3 correspond biologically to two cell fate states, and U_2 is an unstable intermediate state that separates the two basins of convergence. The results here agree well with the previous results on the same system [46], obtained using a much more sophisticated method.

B. A gene regulatory network

We next present a biophysically detailed GRN model of 16 variables, which was derived to understand the mechanism of endogenous circadian rhythm in mammalian cells [48]. (The detailed model equations can be found in the Appendix.) Without control, sustained oscillations of a period of about 24 h can be observed, as shown in Fig. 5(a). When switching control is applied to one of the dynamical variables (M_p), we obtain the biologically significant [48] steady state solution with all components being positive, as shown in Fig. 5(b).

C. Time-delayed Mackey-Glass system

We also study control-based detection of USSs for an infinite-dimensional dynamical system, the time-delayed Mackey-Glass system:

$$\dot{x} = \frac{ax(t - \tau)}{1 + [x(t - \tau)]^b - cx}, \tag{9}$$

where τ is the time delay, and a, b, and c are parameters. This system was originally proposed to model the dynamics of regeneration of blood cells [49], and it has been a paradigmatic model for higher-dimensional nonlinear dynamical systems. For example, for $\tau = 3.18$, $a = 2$, $b = 10$, and $c = 1$, the system exhibits hyperchaos with multiple positive Lyapunov exponents [12]. We apply the following switching control:

$$\dot{x} = \frac{ax(t - \tau)}{1 + [x(t - \tau)]^b - cx} + K(y - x),$$
$$\dot{y} = \omega(t)(x - y), \quad \omega(t) = \omega_{\sigma(t)}, \quad t \in \mathcal{I}_n, \tag{10}$$

where $K = 10$, $\omega_+ = 1$, $\omega_- = -1$, and $\Delta T = 5$. We obtain three USSs, as shown in Fig. 6.

D. Coupled mechanical oscillators

To give an example of physical significance, we consider a system of coupled mechanical oscillators in a parameter regime that exhibits multistability. While a stability analysis of each single oscillator is feasible, to identify all the steady states of coupled oscillators, stable or unstable, is generally a challenging task. To be concrete, we test a pair of bidirectionally coupled dissipationless Duffing oscillators [50]:

$$\dot{x}_1 = x_2, \quad \dot{x}_2 = x_1 - x_1^3 + c_1(y_1 - x_1),$$
$$\dot{y}_1 = y_2, \quad \dot{y}_2 = y_1 - y_1^3 + c_2(x_1 - y_1), \tag{11}$$

where $c_{1,2}$ are coupling coefficients. A single oscillator, without coupling, is a Hamiltonian system with three equilibria and various types of periodic orbits, as shown in Fig. 7(a). With weak coupling there are more unstable equilibria and chaos can arise, as shown in Fig. 7(b). We select x_2 and y_2 to be the variables to implement random switching control.

FIG. 5. (Color online) (a) Dynamics of three mRNA in the circadian rhythm model with sustained oscillation. (b) Convergence to the biologically significant USS with switching control.
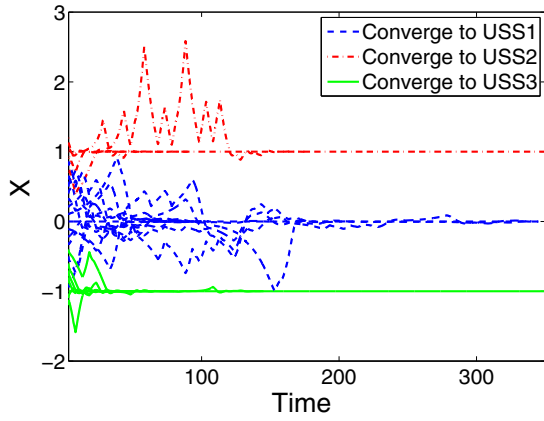
FIG. 6. (Color online) For the Mackey-Glass system with different initial conditions $x(t) \equiv x_0$ for $t \in (-\tau, 0)$, three controlled and detected USSs.

Because of lack of damping, an arbitrarily low value for the cutoff frequency is required. To overcome this difficulty, we implement both linear and derivative feedbacks [21] in the controller, with random switching applied to the linear feedback term only. In total, there are nine unstable equilibria. Starting from different initial conditions, the probabilities of convergence to the nine equilibria are shown in Fig. 7(c). The multistable nature of the system is indicated in Fig. 7(d).

IV. DISCUSSIONS AND CONCLUSIONS

To summarize, we articulate a model-independent random switching control scheme to stabilize and therefore uncover all USSs, regardless of their type, in high-dimensional dynamical systems. The method is mathematically justified using the concept of fast-slow manifold separation and the Markov-chain theory, and numerically validated using examples of biological and physical significance. USSs are particularly important for biological networks, as they are fundamental to phenomena such as cell fate determination. Our control and detection framework may provide a platform to understand biological systems of current interest. Also this framework will be potentially useful for investigating similar problems in fractional dynamical systems [51].

(a)

(b)

(c)

(d)
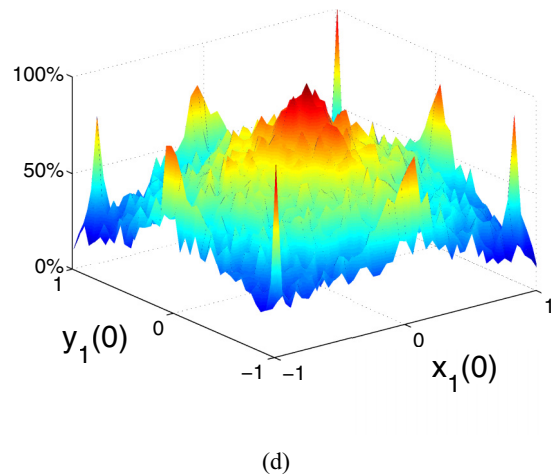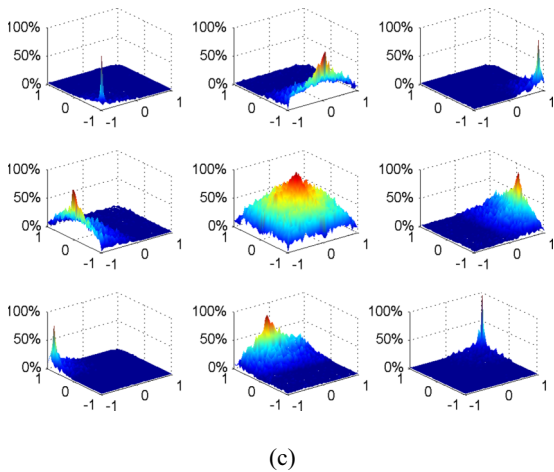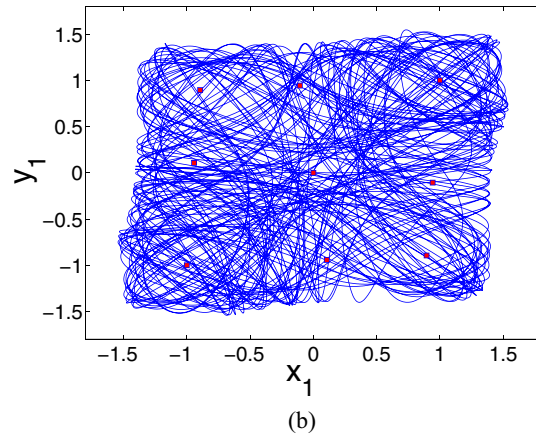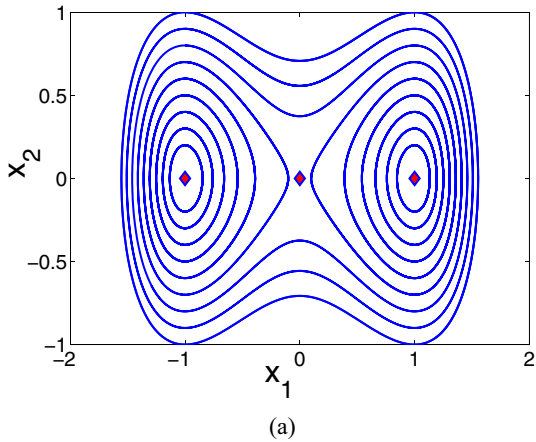
FIG. 7. (Color online) (a) Dynamics of an uncoupled Duffing oscillator with three equilibria. (b) Chaotic behavior in the weakly coupled Duffing oscillator system for $c_{1,2} = 0.1$. Our control method yields all nine unstable equilibria, marked as red squares. (c) The probabilities of convergence to the nine equilibria. (d) Composition of the subplots in (c), where the surface in (d) corresponds to the highest probability from the subplots in (c).

There are a number of issues associated with success of control and detection. First, the switching duration ΔT has a direct effect on control performance. Starting from a random initial condition, from the standpoint of control energy it is desired to find the nearest USS. According to our lemma, the probability ratio for a pair of adjacent USSs is n_+/n_-, where $n_+ = \lceil T_+/\Delta T \rceil$ and $n_- = \lceil T_-/\Delta T \rceil$, and T_+ and T_- are determined by the distances between the starting position and the respective steady states. To approximate T_+/T_- by n_+/n_-, we need to choose the switching window ΔT to be as small as possible to minimize the control energy. However, if ΔT is too small, the expected value of the convergence time, given by $n_- n_+ \Delta T \sim T_- T_+/\Delta T$, will be large. There is thus a tradeoff between control energy and time when choosing the value of ΔT. Second, in our analysis, the dynamical system for $y(t)$ is assumed to be nondegenerate, which is reasonable because a scalar measurement function $g(\boldsymbol{x})$ generally preserves the topological property of the USSs [29]. Third, the quantity $\omega(t)$ in Eq. (3) is the cutoff frequency of the low-pass filter [30], so its absolute value should be smaller than the system damping coefficient. The coupling strength k should be larger than some threshold to stabilize the USSs and to realize the fast-slow manifold separation. To satisfy the threshold requirement, some adaptive schemes for varying k, e.g., $\dot{k} = \sigma[g(\boldsymbol{x}) - y]$, can be considered [52].

To detect USSs and to control the system into a USS are two related issues but they are usually treated separately in the literature. Our random switching scheme represents a unifying scheme to accomplish both tasks in a single framework. Not only that, with respect to each task our scheme has advantages. In fact, our method takes advantage of both stable and unstable filters, while reducing the computational cost. These features can be argued, as follows.

For detection, our random switching framework requires no *a priori* information about the system or the USSs. In particular, compared with the previous proportional or time-delayed feedback control methods [18–20], our method does not require the position of the steady state; it can find the unknown steady state adaptively. In addition, previous works [21–23,25–30] showed that stable filters can detect all USSs of the saddle type, while unstable filters can detect all USSs of the nonsaddle type. In order to detect all USSs, it is necessary to scan through the space of initial conditions twice. However, our random switching scheme is capable of detecting both saddle and nonsaddle types of USSs, requiring searching through the initial condition space only once.

For control of a nonlinear dynamical system, it is generally desired that the system be driven to the nearest steady state in finite time but, with a single stable or unstable filter, this would not be possible since the type and the location of the nearest USS are *a priori* unknown. In contrast, our random switching scheme can adaptively drive the system to the nearest USS with high probability, as exemplified in Fig. 1(c), which is mathematically guaranteed (lemma). Another issue is that, in the situation where there are only saddle type USSs or only

nonsaddle type USSs, a single stable or unstable filter may drive the system into an irrelevant attractor far away from the desirable working region of the phase space, as shown in Fig. 1(e). However, our scheme typically drives the system to some USS near the initial condition with high probability, thereby avoiding any undesirable divergence to some distant attractor.

APPENDIX: A 16-DIMENSIONAL GENE REGULATORY NETWORK

We consider a model for the dynamics of endogenous circadian rhythm in mammalian cells, which consists of 16 kinetic equations [48]. The equations for the three basic variables, namely, mRNA Per, Cry, and $Bmal1$, are

$$\frac{dM_P}{dt} = v_{sP} \frac{B_N^n}{K_{AP}^n + B_N^n} - v_{mP} \frac{M_P}{K_{mP} + M_P} - k_{dmp} M_P,$$

$$\frac{dM_C}{dt} = v_{sC} \frac{B_N^n}{K_{AC}^n + B_N^n} - v_{mC} \frac{M_C}{K_{mC} + M_C} - k_{dmc} M_C,$$

$$\frac{dM_B}{dt} = v_{sB} \frac{K_{IB}^m}{K_{IB}^m + B_N^m} - v_{mB} \frac{M_B}{K_{mB} + M_B} - k_{dmb} M_B.$$

There are also four variables for phosphorylated and nonphosphorylated proteins PER and CRY in the cytosol, which are governed by

$$\frac{dP_C}{dt} = k_{sP} M_P - V_{1P} \frac{P_C}{K_P + P_C} + V_{2P} \frac{P_{CP}}{K_{dp} + P_{CP}}$$
$$+ k_4 PC_C - k_3 P_C C_C - k_{dn} P_C,$$

$$\frac{dC_C}{dt} = k_{sC} M_C - V_{1C} \frac{C_C}{K_P + C_C} + V_{2c} \frac{C_{CP}}{K_{dp} + C_{CP}}$$
$$+ k_4 PC_C - k_3 P_C C_C - k_{dnc} C_C,$$

$$\frac{dP_{CP}}{dt} = V_{1P} \frac{P_C}{K_p + P_C} - V_{2P} \frac{P_{CP}}{K_{dp} + P_{CP}} - v_{dPC} \frac{P_{CP}}{K_d + P_{CP}}$$
$$- k_{dn} P_{CP},$$

$$\frac{dC_{CP}}{dt} = V_{1C} \frac{C_C}{K_p + P_C} - V_{2c} \frac{C_{CP}}{K_{dp} + C_{CP}}$$
$$- v_{dCC} \frac{C_{CP}}{K_d + C_{CP}} - k_{dn} C_{CP}.$$

Next, there are four variables and equations for the phosphorylated and nonphosphorylated PER-CRY complex in the cytosol and nucleus:

$$\frac{dPC_C}{dt} = -V_{1PC} \frac{PC_C}{K_p + PC_C} + V_{2PC} \frac{PC_{CP}}{K_{dp} + PC_{CP}} - k_4 PC_C + k_3 P_C C_C + k_2 PC_N - k_1 PC_C - k_{dn} PC_C,$$

$$\frac{dPC_N}{dt} = -V_{3PC} \frac{PC_N}{K_p + PC_N} + V_{4PC} \frac{PC_{NP}}{K_{dp} + PC_{NP}} - k_2 PC_N + k_1 PC_C - k_7 B_N PC_N + k_8 I_N - k_{dn} PC_N,$$

$$\frac{dPC_{CP}}{dt} = V_{1PC}\frac{PC_C}{K_p + PC_C} - V_{2PC}\frac{PC_{CP}}{K_{dp} + PC_{CP}} - v_{dPCC}\frac{PC_{CP}}{K_d + PC_{CP}} - k_{dn}PC_{CP},$$

$$\frac{dPC_{NP}}{dt} = V_{3PC}\frac{PC_N}{K_p + PC_N} - V_{4PC}\frac{PC_{NP}}{K_{dp} + PC_{NP}} - v_{dPCN}\frac{PC_{NP}}{K_d + PC_{NP}} - k_{dn}PC_{NP}.$$

In addition, there are four variables and equations for the phosphorylated and nonphosphorylated protein $BMAL1$ in the cytosol and nucleus:

$$\frac{dB_C}{dt} = k_{sB}M_B - V_{1B}\frac{B_C}{K_p + B_C} + V_{2B}\frac{B_{CP}}{K_{dp} + B_{CP}} - k_5 B_C + k_6 B_N - k_{dn}B_C,$$

$$\frac{dB_{CP}}{dt} = V_{1B}\frac{B_C}{K_p + B_C} - V_{2B}\frac{B_{CP}}{K_{dp} + B_{CP}} - v_{dBC}\frac{B_{CP}}{K_d + B_{CP}} - k_{dn}B_{CP},$$

$$\frac{dB_N}{dt} = -V_{3B}\frac{B_N}{K_p + B_N} + V_{4B}\frac{B_{NP}}{K_{dp} + B_{NP}} + k_5 B_C - k_6 B_N - k_7 B_N PC_N + k_8 I_N - k_{dn}B_N,$$

$$\frac{dB_{NP}}{dt} = V_{3B}\frac{B_N}{K_p + B_N} - V_{4B}\frac{B_{NP}}{K_{dp} + B_{NP}} - v_{dBN}\frac{B_{NP}}{K_d + B_{NP}} - k_{dn}B_{NP}.$$

Finally, there is an equation describing the inactive complex between $PER\text{-}CRY$ and $CLOCK\text{-}BMAL1$ in the nucleus:

$$\frac{dI_N}{dt} = -k_8 I_N + k_7 B_N PC_N - v_{dIN}\frac{I_N}{K_d + I_N} - k_{dn}I_N.$$

We use the model parameters as in Ref. [48]. Demonstration of successful control to yield the biologically significant USS is shown in the main text.

---

[1] E. Ott, C. Grebogi, and J. A. Yorke, Phys. Rev. Lett. **64**, 1196 (1990).

[2] O. Biham and W. Wenzel, Phys. Rev. Lett. **63**, 819 (1989).

[3] F. K. Diakonos, P. Schmelcher, and O. Biham, Phys. Rev. Lett. **81**, 4349 (1998).

[4] S. M. Zoldi and H. S. Greenside, Phys. Rev. E **57**, R2511 (1998).

[5] R. L. Davidchack and Y.-C. Lai, Phys. Rev. E **60**, 6172 (1999).

[6] P. Cvitanovic, R. L. Davidchack, and E. Siminos, SIAM J. Appl. Dyn. Sys. **9**, 1 (2010).

[7] D. P. Lathrop and E. J. Kostelich, Phys. Rev. A **40**, 4028 (1989).

[8] R. Badii, E. Brun, M. Finardi, L. Flepp, R. Holzner, J. Pariso, C. Reyl, and J. Simonet, Rev. Mod. Phys. **66**, 1389 (1994).

[9] P. So, E. Ott, T. D. Sauer, B. J. Gluckman, C. Grebogi, and S. J. Schiff, Phys. Rev. E **55**, 5398 (1997).

[10] X. Pei, K. Dolan, F. Moss, and Y.-C. Lai, Chaos **8**, 853 (1998).

[11] M. Dhamala, Y.-C. Lai, and E. J. Kostelich, Phys. Rev. E **61**, 6485 (2000).

[12] H. Ma, W. Lin, and Y.-C. Lai, Phys. Rev. E **87**, 050901(R) (2013).

[13] H. Kitano, Nature Rev. Gene. **5**, 826 (2004).

[14] J. Hasty, D. McMillen, and J. J. Collins, Nature (London) **420**, 224 (2002).

[15] L. Bingle, N. J. Brown, and C. E. Lewis, J. Pathol. **196**, 254 (2002).

[16] S. Huang, I. Ernberg, and S. Kauffman, Semin. Cell Dev. Biol. **20**, 869 (2009).

[17] M. Wu, R.-Q. Su, X.-H. Li, T. Ellis, Y.-C. Lai, and X. Wang, Proc. Natl. Acad. Sci. USA **110**, 10610 (2013).

[18] B. Kuo, *Automatic Control Systems* (Prentice-Hall, Upper Saddle River, 1981).

[19] B. Huberman and E. Lumer, IEEE T. Circ. Syst. **37**, 547 (1990).

[20] A. Namajūnas, K. Pyragas, and A. Tamaševičius, Phys. Lett. A **204**, 255 (1995).

[21] G. A. Johnston and E. R. Hunt, IEEE Trans. Circuits Syst. I **40**, 833 (1993).

[22] P. Parmananda, M. A. Rhode, G. A. Johnson, R. W. Rollins, H. D. Dewald, and A. J. Markworth, Phys. Rev. E **49**, 5007 (1994).

[23] D. J. Braun, Phys. Rev. E **78**, 016213 (2008).

[24] W. Lin, Phys. Rev. E **81**, 038201 (2010).

[25] Y. Wu and W. Lin, Phys. Lett. A **375**, 3279 (2011).

[26] W. Lin, H. Ma, J. Feng, and G. Chen, Phys. Rev. E **82**, 046214 (2010).

[27] N. F. Rulkov, L. S. Tsimring, and H. D. I. Abarbanel, Phys. Rev. E **50**, 314 (1994).

[28] K. Pyragas, V. Pyragas, I. Z. Kiss, and J. L. Hudson, Phys. Rev. Lett. **89**, 244103 (2002).

[29] K. Pyragas, V. Pyragas, I. Z. Kiss, and J. L. Hudson, Phys. Rev. E **70**, 026215 (2004).

[30] A. Tamaševičius, E. Tamaševičiūtė, G. Mykolaitis, and S. Bumelienė, Phys. Rev. E **88**, 032904 (2013).

[31] S. W. McDonald, C. Grebogi, E. Ott, and J. A. Yorke, Physica D **17**, 125 (1985).

[32] U. Feudel and C. Grebogi, Chaos **7**, 597 (1997).

[33] U. Feudel and C. Grebogi, Phys. Rev. Lett. **91**, 134102 (2003).

[34] D. Angeli, J. Ferrell, and E. Sontag, Proc. Natl. Acad. Sci. USA **101**, 1822 (2004).

[35] Y.-C. Lai and T. Tél, *Transient Chaos—Complex Dynamics on Finite Time Scales* (Springer, New York, 2011).

[36] X. Ni, L. Ying, Y.-C. Lai, Y.-H. Do, and C. Grebogi, Phys. Rev. E **87**, 052911 (2013).

[37] A. Pisarchik and U. Feudel, Phys. Rep. **540**, 167 (2014).

[38] Y. Guo, W. Lin, and M. Sanjuán, New J. Phys. **14**, 083022 (2012).

[39] J.-Q. Lu, D. W. C. Ho, and L.-G. Wu, Nonlinearity **22**, 889 (2012).

[40] E. N. Lorenz, J. Atmos. Sci. **20**, 130 (1963).

[41] P. J. Menck, J. Heitzig, N. Marwan, and J. Kurths, Nat. Phys. **9**, 89 (2013).

[42] P. J. Menck, J. Heitzig, J. Kurths, and H. J. Schellnhuber, Nat. Comm. **5**, 3969 (2014).

[43] E. Tamaševičiūtė, G. Mykolaitis, S. Bumelienė, and A. Tamaševičius, Commun. Nonlinear Sci. Num. Simu. **19**, 649 (2014).

[44] H. C. Tuckwell, *Elementary Applications of Probability Theory* (Chapman and Hall, London, 1995).

[45] P. Laslo, C. J. Spooner, A. Warmflash, D. W. Lancki, H.-J. Lee, R. Sciammas, B. N. Gantner, A. R. Dinner, and H. Singh, Cell **126**, 755 (2006).

[46] N. Radde, BMC Syst. Biol. **6**, 57 (2012).

[47] N. Radde, Bioinformatics **26**, 2874 (2010).

[48] J.-C. Leluop and A. Goldbeter, J. Theo. Bio. **230**, 541 (2004).

[49] M. C. Mackay and L. Glass, Science **197**, 287 (1977).

[50] J. Guckenheimer and P. Holmes, *Nonlinear Oscillations, Dynamical Systems, and Bifurcations of Vector Fields* (Springer, New York, 1983).

[51] X. Ji, W. Yu, W. Sheng, and W. Lin, Chaos **24**, 023119 (2014).

[52] H.-F. Ma and W. Lin, SIAM J. Control Opt. **51**, 3692 (2013).